NASA Technical Memorandum 104428
AIAA-91-3354

Evaluation of Panel Code Predictions With Experimental Results of Inlet Performance for a 17-Inch Ducted Prop/Fan Simulator Operating at Mach 0.2

D.R. Boldman, C. Iek, D.P. Hwang,
and R.J. Jeracki
Lewis Research Center
Cleveland, Ohio

and

M. Larkin and G. Sorin
Pratt and Whitney Aircraft
East Hartford, Connecticut

Prepared for the
27th Joint Propulsion Conference
cosponsored by the AIAA, SAE, ASME, and ASEE
Sacramento, California, June 24-27, 1991

NASA

EVALUATION OF PANEL CODE PREDICTIONS WITH EXPERIMENTAL RESULTS OF INLET PERFORMANCE FOR A 17-INCH DUCTED PROP/FAN SIMULATOR OPERATING AT MACH 0.2

D. R. Boldman[1], C. Iek, D. P. Hwang, and R. J. Jeracki
National Aeronautics and Space Administration
Lewis Research Center
Cleveland, Ohio 44135

M. Larkin and G. Sorin
Pratt and Whitney Aircraft
East Hartford, Connecticut 06108

Abstract

An axisymmetric panel code was used to evaluate the performance of a series of ducted propeller inlets which were designed by P&W Aircraft and tested in the NASA Lewis 9- by 15-Foot Low Speed Wind Tunnel as part of a joint program with P&W Aircraft. Three basic inlets having ratios of shroud length to propeller diameter of 0.2, 0.4, and 0.5 were tested with the P&W ducted prop/fan simulator. A fourth "hybrid" inlet consisting of the shroud from the shortest basic inlet coupled with the spinner from the longest basic inlet was also tested. This latter configuration represented the shortest overall inlet. The simulator duct diameter at the propeller face was 17.25 inches. The short and long spinners provided hub-to-tip ratios of 0.44 at the propeller face. The four inlets were tested at a nominal free stream Mach number of 0.2 and at angles-of-attack from 0° to 35° (upper limit of the model support system). The panel code method incorporated a simple two-part separation model which yielded conservative estimates of inlet separation.

Nomenclature

A	area
C_f	friction coefficient
D	diameter
L	shroud length
M	Mach number
p	static pressure
P	total pressure
V	velocity
W	mass flow rate
X	axial distance from propeller face
α	angle-of-attack
ρ	density

Subscripts

c	corrected to standard day conditions
i	incompressible value
LOC	local condition
MAX	maximum value
0	total condition
PROP	propeller face
S	static condition
cor	corrected for compressibility

Superscript

–	average value

Background

Panel codes have been demonstrated to be powerful tools for the design of a variety of subsonic inlets including short inlets for VTOL and STOL aircraft operating at high angles-of-attack[1-2] (often approaching 90°). Panel methods have been extended to include complex 3-D geometries with and without slats[3-8] and have yielded good predictions of the surface static pressures at conditions in which the inlet was operating free of separated flow. In many of the applications panel codes were compared to data from inlets where the pumping of the flow was achieved by some external means rather than by an integral propeller or fan. In other related experiments in which an integral fan was used to pump the flow, the inlets were relatively long ($X/D_{FAN} > 0.5$). In either case the pumping mechanism probably did not exert a strong influence on the inlet flow. Consequently, the panel codes, which do not account for the presence of a fan or propeller (except through the mass flow rate), would be expected to yield good predictions of the

[1]Aerospace Research Engineer
Assoc. Fellow AIAA

surface pressures inside the inlet, particularly when the inlet was free of separated flow. In the present paper, the Douglas-Neumann panel code EOD[9-11] in conjunction with SCIRCL[12] and COMBYN[12] were used to predict the inlet static pressures and separation observed in recent tests with the P&W ducted prop/fan simulator. The code COMBYN incorporated a compressibility correction. A boundary layer calculation, which will be described later, was added to COMBYN in order to predict diffuser separation. This unique data base provided an excellent opportunity to re-examine the panel code for subsonic inlet design since the inlet local Mach number levels were often perceived to be too high for this class of design codes.

In comparing the panel code results with inlet data from the simulator, emphasis has been placed on (1) the comparison of inlet surface static pressures on the windward side as the angle-of-attack approached the separation value, and (2) the comparison of predicted and observed angle-of-attack corresponding to the "onset" of separation.

Panel Code

Potential Flow

Since the theory for the panel code is well documented[12], only a brief description of the method will be given. The basic problem consists of calculating the potential flow (with a correction for compressibility effects) about an axisymmetric ducted propeller inlet at any combination of inlet mass flow, W_c, and inlet angle-of-attack, α. A series of programs developed at NASA Lewis Research Center in the early seventies are used to solve this problem. The first program, SCIRCL, represents the axisymmetric inlet geometry by its meridional profile with the shroud and spinner extended far downstream in order to obtain an accurate potential flow solution in the region between the highlight and propeller face. SCIRCL breaks the profile into segments with a control point on each segment used for the potential flow calculations. The program also generates off-body points such as flow measuring rakes at prescribed axial stations. One such rake station represents a "control" station for subsequent use in the COMBYN program.

The Douglas-Neumann program, EOD[9-11], provided the fundamental incompressible potential flow field for the geometry specified by SCIRCL. In EOD, three basic flow conditions are computed; namely, a static condition ($M_0 = 0$), and two stream flow conditions with unity velocity vectors parallel to each of the two cartesian coordinate axes. The X-axis represents the axial direction for zero angle-of-attack. The basic solutions are obtained by replacing the surface by a number of panels having a surface source (or sink) distribution of unknown strength. In the present applications, a piecewise-parabolic source strength distribution was assumed in conjunction with a higher order calculation which uses curved surface elements. A distribution of unit vortices on the shroud surface is used to induce a static mass flow through the inlet (in addition to the distribution of sources that represent the inlet profile). Arbitrary static mass flows are obtained by using a multiplication factor.

The basic solutions obtained from EOD are combined linearly in a program called COMBYN to provide solutions of interest for the prescribed flow conditions, free stream Mach number, angle-of-attack, and mass flow. The linearly combined incompressible solution is corrected for compressibility by the Lieblein-Stockman[13] compressibility correction. This correction, simply stated, is

$$V_{cor} = V_i \times \left(\frac{\rho_O}{\rho_S} \right)^{\frac{V_i}{V_t}} \qquad (1)$$

where the terms on the right side are obtained from the input conditions and the incompressible flow solution. The other desired properties such as Mach number and pressure ratio are obtained from the compressible velocity, V_{cor}.

The solutions from COMBYN require the specification of a control station which, in the present study, was chosen to be the throat of the inlet. Since the compressibility correction does not exactly satisfy continuity, the COMBYN solutions are most accurate near the control station (or near the throat region in the present application).

Boundary Layer and Separation Model

The code capability as described above allows for the calculation of the inlet static pressure distribution upon accounting for compressibility. It now remains to determine the maximum angle-of-attack that can be obtained prior to boundary layer separation in the inlet. Several empirically based separation models have been used in the past with varying degrees of success[14-15]. The separation model used in this paper is based, in part, on experimental observations from past studies of inlets

operating at high angles-of-attack and at flow rates sufficiently high to produce locally supersonic flow in the internal lip region of the windward side of the inlet. Based on these past experiments, it was concluded that a shock-induced lip separation of the internal flow in the shroud could be expected when the Mach number reached a value of about 1.5[14]. However, if the Mach number remains below 1.5, separation of the boundary layer can still occur in the diffuser starting near the exit or propeller face and moving upstream with an increasing adverse pressure gradient resulting from an increasing angle-of-attack. These two observations were combined to provide the simple separation model used in the present study. This model is depicted in Fig. 1. The first limiting condition in climb angle-of-attack arises when the Mach number limit of 1.5 is exceeded as shown in Fig. 1a. The second condition which can limit the climb angle-of-attack is when the local Mach number does not reach a value of 1.5 but separation occurs in the diffuser (C_f = 0) as suggested in Fig. 1b. Since the panel code model of the inlet is based on a flow-through duct extending far downstream, the calculated boundary layer can separate anywhere inside the long duct. For purposes of identifying the diffusion-limited angle-of-attack, it is assumed that this limit is reached when the calculated separation occurs upstream of the diffuser exit. The diffuser exit is defined as the plane representing the location of the propeller face.

The analysis of the boundary layer is based on the 2-dimensional compressible boundary layer program of Herring[16]. This numerical method calculates the usual boundary layer parameters including the skin friction coefficient, C_f . Flow separation occurs when C_f = 0. The program contains several options for controlling the boundary layer development including the initialization and transition criterion. A fixed set of assumptions were made concerning the boundary layer options and no effort was made to alter these options for the results presented herein.

3-D Euler Code

In addition to the panel code predictions, a few comparisons of the inlet static pressure distributions were made with a 3-D version of an Euler flow solver developed by Ni[17]. The Euler flow solver uses a fast explicit numerical scheme for solving the unsteady Euler flow equations to obtain steady solutions. The scheme is constructed by combining the multiple grid technique with a second order accurate finite volume integration method. Comparisons between the panel code, 3-D Euler code, and data were made for the conventional inlet.

Experimental Rig

Installation

The P&W 17-in. diameter ducted propeller simulator was installed in the 9- by 15- Foot Low Speed Wind Tunnel as shown in Fig. 2. The centerline of the simulator was 51 in. from the tunnel floor and was offset 21 in. in a lateral direction from the tunnel centerline. This offset resulted in a model centerline which was 65 in. from the near wall of the tunnel and 113 in. from the far wall. The simulator was rotated about the pivot axis in a counterclockwise direction to increase the angle-of-attack, i.e. an increasing angle-of-attack was obtained as the model was rotated laterally toward the wind tunnel centerline. The maximum angle-of-attack for the support system was 35°. The propeller was driven by a 1,000 HP air turbine drive system at rotational speeds up to 12,000 RPM.

Inlets

The inlets which were tested on the ducted propeller simulator are shown in Fig. 3. These inlets were assembled from three different shrouds and two spinners. The shorter of the two spinners had a length approximately equal to the length of the conventional shroud (0.5 D_{PROP}). The longer spinner had a length of about 0.7 D_{PROP} and was used only with the shortest shroud to form the "plug" inlet shown in Fig. 3d. The short spinner was also combined with the three shrouds to form the "conventional", "hybrid", and "midlength" inlets shown in Figs. 3a to 3c, respectively. The inlet lengths based on the ratio of shroud length to propeller diameter ranged from 0.2 to 0.5.

Instrumentation

The simulator was extensively instrumented throughout the flow path in order to provide data for this multipurpose program in which the present inlet results comprised only a small but important part. Static pressure taps, thermocouples for health monitoring and rakes, rake total pressures, and blade clearance proximity probes accounted for nearly 550 channels of steady state data. Several additional types of instrumentation for dynamic measurements and acoustics were included to support other aspects of the program. The inlet results presented in this paper were based primarily on measure-

ments of surface static pressures on the windward side of the inlets, total pressure contours for assessing the degree of distortion ahead of the propeller, angle-of-attack, captured mass flow rate, and free stream conditions.

Emphasis has been placed on the data obtained at angles-of-attack above about 25° where inlet separation starts to become a concern. The number of static pressure measurements in the inlet ranged from 9 for the short shroud to 14 for the midlength shroud. The spacing between pressure taps was designed to provide good resolution in the highlight region where shock-induced separation can occur. The concentration of pressure taps in this region will become apparent upon examining the pressure distributions presented in the section entitled **Results**.

The inlet total pressure distortion profiles were obtained from four rakes, each containing 12 tubes. Distortion profiles will be presented for the midlength inlet with the rakes located 3.0 in. upstream of the propeller face. The tube spacing ranged from 0.5 in. near the spinner to 0.23 in. near the shroud. The tube nearest the shroud was displaced 0.06 in. from the surface. The rakes were positioned circumferentially at 0° (leeward side), 20°, 170°, and 185° (representing the windward side). Symmetry was assumed about the 0° - 180° axis. This symmetry assumption coupled with an interpolation program provided an additional nine pseudo rakes which were used to estimate the total pressure contours.

Test Conditions

Results are presented for a nominal free stream Mach number of 0.2. The tests were performed over an angle-of-attack range of 0° to 35° and at corrected speeds of 7,500 to 12,000 RPM. Corrected flows ranged from nominal values of 30.5 to 45.5 lb/sec. In the comparisons between experiment and theory, the experimental values of corrected mass flow were used in the theory rather than the nominal values. These experimental values may vary by about ± 1 lb/sec from the nominal values given above.

Results

Panel Code vs. 3-D Euler Predictions, Conventional Inlet

The results of panel and 3-D Euler code predictions of the inlet static pressure distributions for the conventional inlet are shown in Fig. 4. These results are for three angles-of-attack ranging from 25.0° (Fig. 4a) to 27.3° (Fig 4c). At α = 25.0°, the observed minimum value of p/P_0 reaches a value of 0.27 which corresponds to a local Mach number of 1.5 (Fig. 4a). At the higher values of α, the experimental minimum pressure ratio starts to increase resulting in lower peak values of local Mach number (Figs. 4b and 4c). Both the axisymmetric panel and 3-D Euler codes yield excellent agreement with each other and with the data at α = 25.0° where the experimental peak Mach number was observed. At higher angles-of-attack where the peak Mach number starts to drop (minimum value of p/P_0 increases), the two codes continue to predict higher values of peak Mach number since viscous effects are not included in the codes.

The results of these comparisons indicate that the potential flow code (with a compressibility correction) provides excellent agreement with the 3-D Euler code at conditions where separation has not occurred. Also, both codes yield excellent agreement with the data for the conventional inlet up to the angle-of-attack where the flow separates.

Panel Code Predictions vs. Experiment, Shorter Inlets

The panel code calculations were extended to include the other three inlets operating at the highest mass flow rate. The predicted inlet static pressure distributions for the hybrid, midlength, and plug inlets are compared with the experimental results in Figs. 5 to 7. The experimental peak values of local Mach number increased relative to the value obtained in the conventional inlet and permitted separation-free operation at much higher angles-of-attack as shown in Figs. 5 and 7. This can be noted by comparing the experimental minimum values of p/P_0 to the value of 0.27 which corresponds to a Mach number of 1.5. The local Mach numbers for the short shroud hybrid and plug configurations reached levels of 1.65 at angles-of-attack of 34.3°. At slightly higher values of α, full separation can be noted by an abrupt increase in the minimum value of static pressure followed by a flattening of the internal pressure distribution (Figs. 5c and 7c). The midlength inlet peak Mach number reached 1.5; however this Mach number was attained at α = 29.0° rather than at 25.0° which was observed for the conventional inlet. Again, the panel code predictions of static pressure were generally in good agreement with experimental results up to the point of separation. Close examination of Figs. 5

to 7 reveals a slightly lower predicted minimum static pressure than observed experimentally; however, in view of the difficulty in obtaining higher experimental resolution of the pressures in the highlight region, it cannot be determined whether these differences are real or whether the true minimum in static pressure was not measured because it may not have occurred precisely at the location of a static tap.

Experimental Separation

In order to perform comparisons between predicted and experimental separation, consideration must be given to the method of determining, from the measurements, when separation has occurred in the inlet. In the preceding discussion, Figs. 5c and 7c were presented to show the static pressure distribution in a fully separated inlet, i.e. an inlet which separates at the lip. In these cases, the inlet exhibits a normal (unseparated) type of pressure distribution at an angle-of-attack of only about one degree less than the value associated with lip separation. In other words, the lip separation occurs rather abruptly after some limiting value of α is reached. This type of separation generally occurred at the high corrected mass flow operating condition. For purposes of selecting an experimental lip separation criterion, this limiting value of α was assumed to be the angle-of-attack where the highest value of inlet local Mach number is obtained. This criterion was also applied to the results obtained at the low mass flow rates to determine when separation occurred in the diffuser. Experimental support for these assumptions will be provided below.

First, consider the distributions of $M_{LOC,MAX}(\alpha)$ for the midlength inlet in Fig. 8. Two sets of distributions are provided to show (1) the influence of inlet rakes on the results, and (2) the reduction of $M_{LOC,MAX}$ with an increase in α after the peak Mach number is reached. The influence of the rakes can be noted by comparing Figs. 8a and 8b. The distributions of $M_{LOC,MAX}(\alpha)$ are essentially the same except for a slight increase in the limiting value of α when the rakes were installed. The presence of the rakes, located 3.0 inches upstream of the propeller face, can increase the separation angle-of-attack in two ways. First of all, the blockage from the rakes changes the diffusion rate in the inlet which may delay the separation. A second factor concerns the turbulence generated by the rakes which energizes the diffuser boundary layer and delays separation. All of the results, with the exception of the inlet total pressure contours, were obtained with the rakes removed.

As indicated above, the value of α corresponding to the maximum value of $M_{LOC,MAX}(\alpha)$ was selected as the limiting angle-of-attack for a separation-free inlet. In Fig. 8b, the distributions of $M_{LOC,MAX}(\alpha)$ at low and high corrected flows show a distinct peak value of $M_{LOC,MAX}$. However, the distribution at the low corrected flow does not exhibit the pronounced drop in Mach number that was characteristic of the results at high flow rates. Although the decrease in $M_{LOC,MAX}$ after the peak value is more gradual with lower flows, separation is still present in the inlet. This separation occurs in the diffuser and, as shown below, the extent of this separated region tends to increase with increasing angle-of-attack until the inlet becomes fully separated.

Lip separation and diffuser separation can be observed in the midlength inlet by comparing the distributions of $M_{LOC}(X)$ at the limiting values of α and at angles greater than the limiting values. Two such distributions are shown in Fig. 9 for the highest flow condition. In Fig. 9a the distribution is shown for α = 28.3° which corresponds to a peak value of $M_{LOC,MAX}$ of 1.51 (Fig. 8b). The inlet Mach number distribution shown in Fig. 9b corresponds to a slightly higher α of 29.9° and indicates full separation emanating from the lip of the inlet. This separation is evident from the relatively flat distribution of Mach number over the entire inlet. On the basis of this illustration for the midlength inlet, the maximum value of $M_{LOC,MAX}(\alpha)$ appears to represent a proper criterion for determining the limiting angle-of-attack for the prevention of separation (lip separation in this illustration).

The second type of separation; namely, diffuser separation, occurs when the peak inlet Mach number is less than 1.5 but a peak value appears in the $M_{LOC,MAX}(\alpha)$ distribution. Such a condition is apparent in the low flow results shown in Fig. 8b. The inlet Mach number distributions for three angles-of-attack at and above the limiting value are shown in Fig. 10. In Fig. 10a the inlet Mach number distribution is shown for α = 28.4° which corresponds to a peak value of $M_{LOC,MAX}$ of 0.80 (Fig. 8b). Separation is not evident because the local Mach number continuously decreases without regions of constant Mach number which would suggest separation. In Fig. 10b the distribution is shown for α = 30.1°. Two changes become apparent. First of all, the peak Mach number has decreased. Secondly, a region ($-5 < X < -4$) of constant Mach number, representing separation, appears in the diffuser. The extent of this separation increases with increasing angle-of-attack until finally, the inlet becomes fully separated. This condition, shown in

Fig. 10c, occurs at an angle-of-attack of 32.4°.

In Figs. 9 and 10, separation was determined on the basis of a region of constant Mach number in the inlet. Additional support for selecting the separation angle on the basis of a peak value in the $M_{LOC,MAX}(\alpha)$ distribution can be provided if one considers the reason for the drop in $M_{LOC,MAX}$ when separation is present. Before the onset of inlet separation, at a given angle of attack, the high rate of flow curvature around the lip reduces the static pressure indicating high values of surface Mach number. As the inlet angle-of-attack is increased, lip separation begins to occur causing a reduced rate of curvature and results in lower levels of Mach number. As the angle-of-attack continues to increase, the separation region grows until there is very little or no lip acceleration. In addition, the inlet separation produces a total pressure loss which, for a given fan speed line, reduces fan corrected flow and further reduces the inlet surface Mach number.

Distributions of $M_{LOC,MAX}(\alpha)$ are shown in Figs. 11 to 14 for the four inlets with the inlet rakes removed. Each figure shows the distributions at the low and high corrected flow rates. A maximum in these distributions occurs at the high mass flow rates in all of the inlets. This maximum was not reached with the short shroud inlets operating at low flow rates because of the 35° angle-of-attack limit of the test stand (Figs. 12 and 14). A maximum was not obtained for the conventional inlet operating at the low mass flow rate (Fig. 11) because of high propeller strain levels possibly caused by diffuser separation.

Inlet Total Pressure Contours, Midlength Inlet

Inlet total pressure contours for the midlength inlet are shown in Figs. 15 and 16 for the lowest and highest corrected mass flow rates, respectively. Very little total pressure deficit can be observed at the low flow condition, even at an α of 31.2° which is beyond the angle of peak Mach number (refer to Fig. 8a). It will be shown later that separation in the diffuser was predicted for these low flow, high α conditions. The results in Fig. 16, obtained at the high flow rate, show little total pressure deficit at angles up to 29.9°; however, a pronounced distortion is apparent at a slightly higher α of 31.3°. As shown in Fig. 8a, these angles correspond to the peak Mach number condition and a condition where $M_{LOC,MAX}$ has experienced a rapid drop.

Predicted Separation Based on Simple Model

The two-part separation model shown in Fig. 1 was incorporated in the panel code to provide estimates of the separation angle-of-attack. Results for the four inlets are shown in Fig. 17 where the separation angle-of-attack is plotted as a function of the specific flow at the propeller face. The region under the solid line for each inlet represents the conditions for separation-free inlet operation. The dashed line is an extension of the predicted diffuser separation (C_t = 0). This line would represent the predicted separation if the separation model did not contain the Mach 1.5 limitation. Diffuser separation was the dominant limiting factor at the lower values of specific flow. The calculations suggested that the highest angles-of-attack could be achieved with the short shroud inlets (hybrid and plug). Predictions for the midlength and conventional inlets showed a difference of only about 2° in diffuser separation angle-of-attack with the midlength inlet predicted to yield slightly higher values of separation angle. Similar trends are apparent in the curves representing the Mach 1.5 limitation; however these lines indicate a rather pronounced reduction in separation angle with increasing flow rate.

Predicted vs. Experimental Separation

Fig. 18 shows the results of experimental separation superimposed on the results of the predicted separation which were shown in Fig. 17. The simple separation model yields reasonable predictions of the separation for the conventional, hybrid, and midlength inlets (Figs. 18a, 18b, and 18c, respectively) with a general tendency to underpredict the experimental separation angle. The results for the plug inlet, shown in Fig. 18d, tend to be the most conservative, particularly at the highest flow rates. One of the reasons concerns the Mach 1.5 limitation at the high flows. As noted earlier, the short shroud inlets operated with peak Mach numbers as high as 1.65. If the short shroud results for the hybrid and plug inlets are compared, the panel code with the separation model suggests that higher angles should be achievable with the hybrid inlet (Fig. 17). However, if the experimental results are compared for these inlets (Figs. 18b and 18d) little difference can be detected. The differences in the calculated results must be related to the difference in spinner geometry. The panel code indicated slightly higher separation-free angles-of-attack with the hybrid inlet which contained the short spinner. However, the experiment indicated little effect of the spinner on the shroud pressure distributions.

The results in Fig. 18 suggest that the separation angle-of-attack might be represented exclusively by the calculated results based on the boundary layer analysis since the data and the analysis both reveal only modest reductions in the separation angle with increasing specific flow. On the other hand, the lip separation curves based on a limiting Mach number of 1.5, indicate a rapid decline in the limiting angle-of-attack at high specific flows. This criterion provided conservative estimates of lip separation for the inlets of this investigation. It is recognized that the Mach 1.5 limit was based on an average of the results from several inlets[14] which fell within a Mach number band of about 1.5 ± 0.15. Indeed, the present results for the short inlets indicated that the local Mach number can be as high as 1.65 without separation. However, as the specific flow increases, lip separation will eventually occur, and the rapid drop in separation angle-of-attack represented by the Mach 1.5 limiting lines would be expected. Consequently, in utilizing panel codes for the design of inlets for large ADP systems, which might require higher specific flows, a conservative approach of maintaining the Mach 1.5 limit in the simple separation model is recommended.

Concluding Remarks

The results for the hybrid and plug inlets, which contained a short shroud (L/D_{PROP} = 0.2), revealed surprisingly good aerodynamic climb performance. These short inlets were able to support local Mach numbers as high as 1.65 without incurring lip separation, whereas the longer conventional and midlength inlets were limited to local Mach numbers of about 1.5. The reason for these differences is still unclear; however, it is believed to be associated with the pumping effect of the propeller. The influence of the propeller would tend to become more dominant as the inlet becomes shorter.

Summary

An axisymmetric panel code was used to evaluate the performance of a series of ducted propeller inlets which were designed by P&W Aircraft and tested in the NASA Lewis 9- by 15-Foot Low Speed Wind Tunnel as part of a joint program with P&W Aircraft. Four inlets, with ratios of shroud length to propeller diameter of 0.2 to 0.5, were tested with the P&W 17-in. ducted prop/fan simulator. A short and long spinner were used in various combinations with the shrouds. These spinners provided hub-to-tip ratios of 0.44 at the propeller face. The tests were performed at a free stream Mach number of 0.2 and at angles-of-attack from 0° to 35°.

A panel method involving a series of codes was used to predict the inlet pressure distributions and separation angle-of-attack. Limited calculations indicated that the panel code results for the inlet static pressure distribution were in good agreement with 3-D Euler predictions at angles-of-attack approaching the separation value. The panel code was used in conjunction with a simple two-part model to predict separation. This model, consisting of a boundary layer separation calculation (C_f = 0) and a limiting Mach number criterion, yielded good estimates of the inlet separation over most of the operating range. The results were generally conservative, especially at high flow conditions. At high flow rates, the local Mach number limit of 1.5 used in the model, was too low for the short shroud inlets. Experiments for these inlets indicated separation-free operation with local Mach numbers as high as 1.65.

References

1. Hawk, J. D., and Stockman, N. O., "Theoretical Study of VTOL Tilt-Nacelle Axisymmetric Inlet Geometries," NASA TP-1380, Jan. 1979.

2. Boles, M. A., Luidens, R. W., and Stockman, N. O., "Theoretical Flow Characteristics of Inlets for Tilting-Nacelle VTOL Aircraft," NASA TP-1205, April 1978.

3. Hwang, D. P., and Diedrich, J. H., "A Summary of V/STOL Inlet Analysis Methods," NASA TM-82725, Dec. 1981.

4. Hwang, D. P., and Abbott, J. M., "A Summary of V/STOL Inlet Analysis Methods," NASA TM-82885, Aug. 1982.

5. Hwang, D. P., "A Numerical Analysis Applied to High Angle-of-Attack Three-Dimensional Inlets," AIAA-86-1627, June 1986.

6. Kao, H. C., "Some Aspects of Calculating Flows About Three-Dimensional Subsonic Inlets, NASA TM-82678, July 1981.

7. Hess, J. L., Mack, D. P., and Stockman, N. O., "An Efficient User-Oriented Method for Calculating Compressible Flow in and About Three-Dimensional Inlets - Panel Method," NASA CR-159578, April 1979.

8. Hess, J. L., Friedman, D. M., and Clark, R. W., "Calculation of Compressible Flow About Three-Dimensional Inlets with Auxiliary Inlets, Slats, and Vanes by Means of a Panel Method," NASA CR-174975, June 1985.

9. Smith, A. M. O., and Pierce, J., "Exact Solution of the Neumann Problem. Calculation of Non-Circulatory Plane and Axially Symmetric Flows About or Within Arbitrary Bodies," ES-26988, Douglas Aircraft Co., April 1958.

10. Hess, J. L., and Smith, A. M. O., "Calculation of Potential Flow About Arbitrary Bodies," Progress in Aeronautical Sciences, Vol. 8, D. A. Kuchemann, ed., Pergamon Press, Elmsford, NY, 1967, pp. 1-138.

11. Hess, J. L., "Calculation of Potential Flow About Bodies of Revolution Having Axes Perpendicular to the Free-Stream Direction," Journal of the Aerospace Sciences, Vol. 29, No. 6, June 1962, pp. 726-742.

12. Stockman, N. O., and Farrell, Jr., C. A., "Improved Computer Programs for Calculating Potential Flow in Propulsion System Inlets," NASA TM-73728, July 1977.

13. Lieblein, S., and Stockman, N. O., "Compressibility Correction for Internal Flow Solution," Journal of Aircraft, Vol. 9, April 1972, pp 312-313.

14. Luidens, R. W., Stockman, N. O., and Diedrich, J. H., "Optimum Subsonic, High-Angle-of-Attack Nacelles," ICAS Proceedings 1980, 12th Congress of the International Council of the Aeronautical Sciences, Oct. 1980, Munich/Federal Republic of Germany, edited by J. Singer and R. Staubenbiel, AIAA, 1980, pp. 530-541.

15. Burley, R. R., "Experimental Investigation of Tangential Blowing Applied to a Subsonic V/STOL Inlet," NASA TP-2297, April 1984.

16. Herring, H. J., "PL2 - A Calculation Method for Two-Dimensional Boundary Layers with Cross-flow and Heat Transfer," Dynalysis of Princeton, Report No. 65, July 1980.

17. Ni, Ron-Ho, "A Multiple Grid Scheme for Solving the Euler Equations," AIAA-81-1025, June 1981.

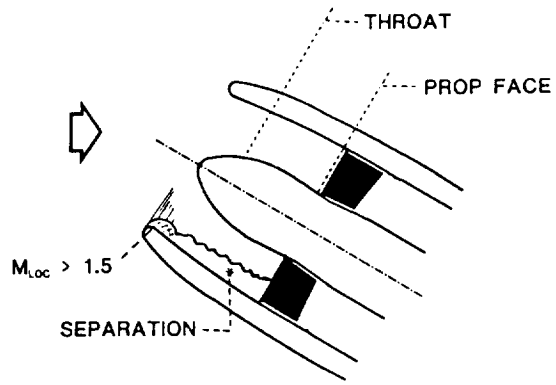

a. Mach Number Limited

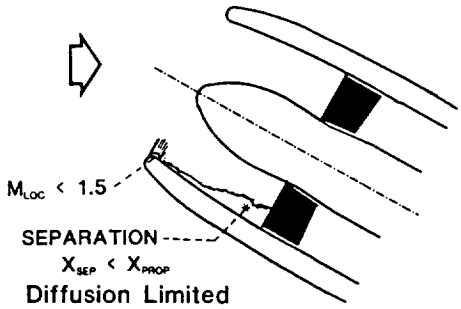

b. Diffusion Limited

Fig 1 Separation model used in conjunction with the panel code to establish separation-free operating regime.

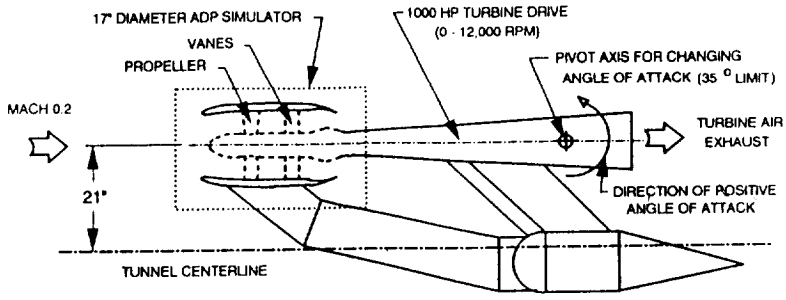

TOP VIEW

Fig 2 Installation of 17-Inch Advanced Ducted Propeller simulator in the 9' X 15' Low Speed Wind Tunnel.

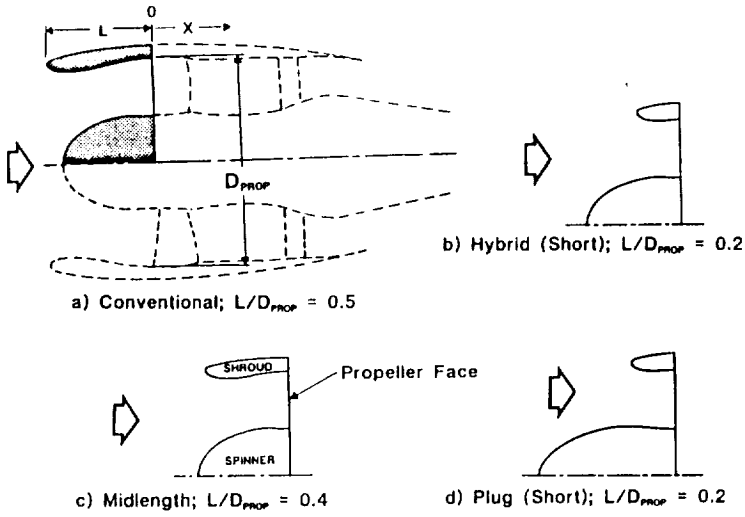

Fig 3 Schematic representation of the ADP inlets; D_{PROP} = 17.25 in.

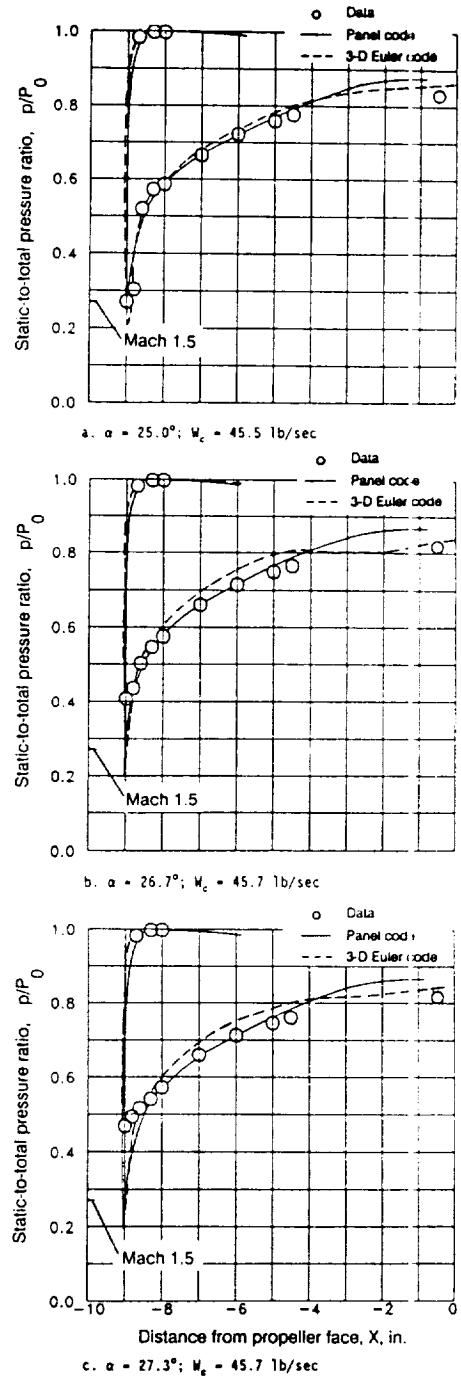

Fig 4 Comparison of predicted windward side static pressures with experiment for the conventional inlet at angles of attack approaching separation.

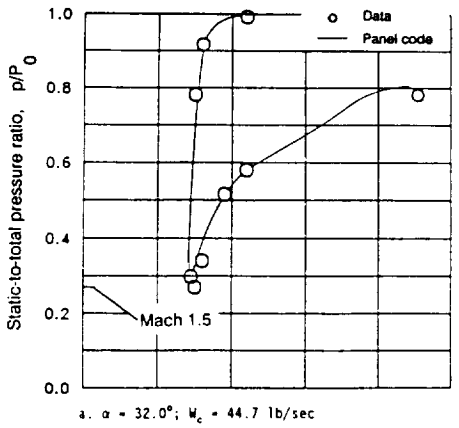

a. α = 32.0°; W_c = 44.7 lb/sec

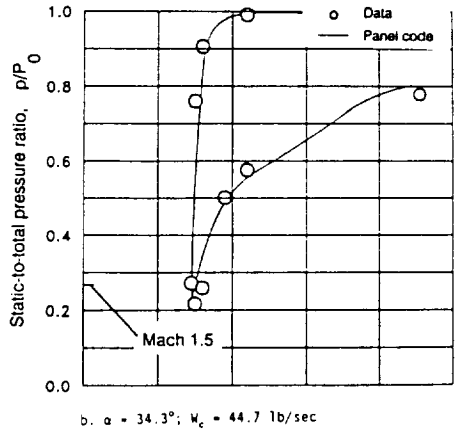

b. α = 34.3°; W_c = 44.7 lb/sec

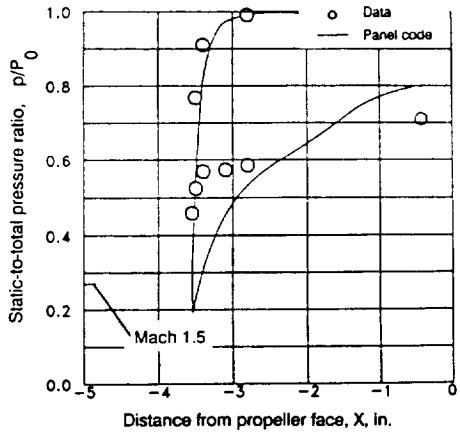

c. α = 35.7°; W_c = 44.7 lb/sec

Fig 5 Comparison of predicted windward side static pressures with experiment for the hybrid inlet at angles of attack approaching and

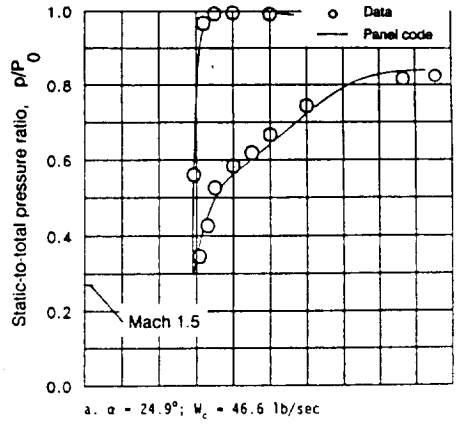

a. α = 24.9°; W_c = 46.6 lb/sec

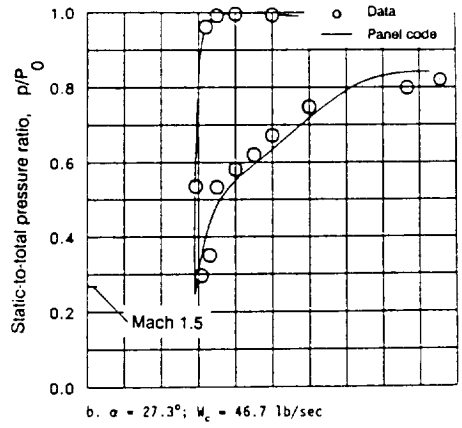

b. α = 27.3°; W_c = 46.7 lb/sec

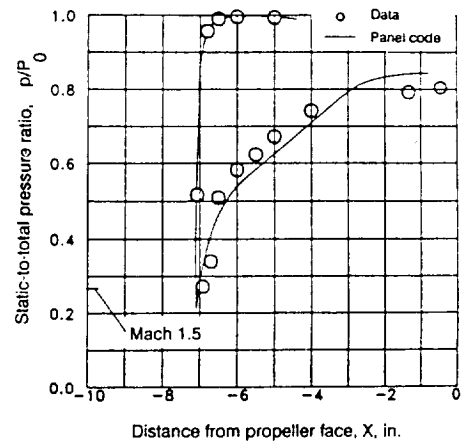

c. α = 29.0°; W_c = 46.8 lb/sec

Fig 6 Comparison of predicted windward side static pressures with experiment for the midlength inlet at angles of attack approaching separation.

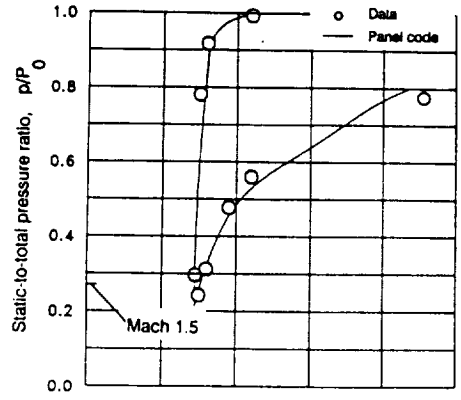

a. α = 32.0°; W_c = 44.7 lb/sec

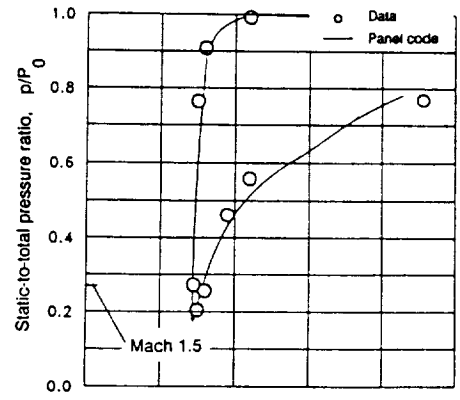

b. α = 34.3°; W_c = 44.7 lb/sec

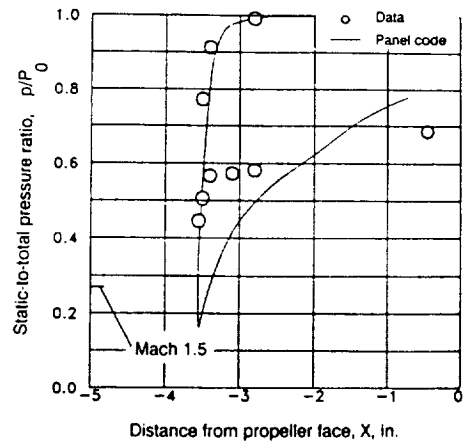

c. α = 35.7°; W_c = 44.7 lb/sec

Fig 7 Comparison of predicted windward side static pressures with experiment for the plug inlet at angles of attack approaching and during full separation.

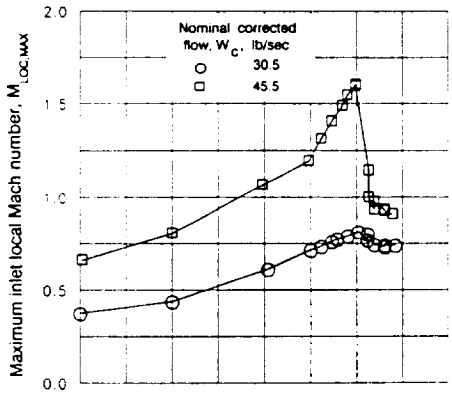

a. Inlet rakes installed

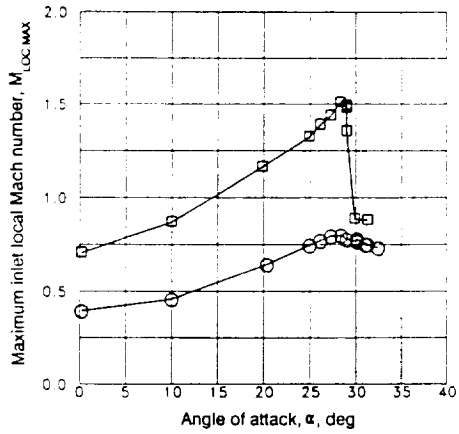

b. Inlet rakes removed

Fig 8 Influence of inlet rakes on the maximum local Mach number in the midlength inlet.

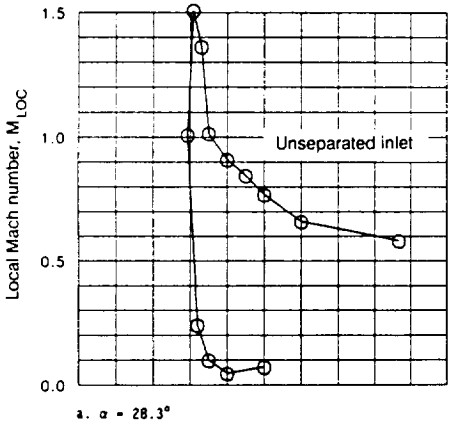

a. α = 28.3°

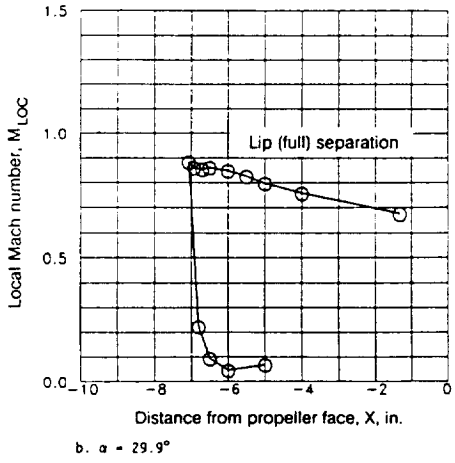

b. α = 29.9°

Fig 9 Inlet Mach number distributions in the midlength inlet showing the development of lip separation. Nominal corrected flow, W_c, 45.5 lb/sec.

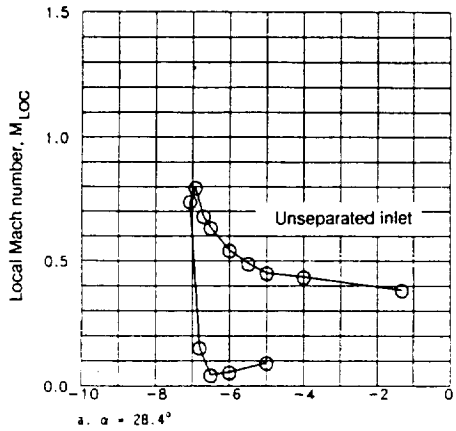

a. α = 28.4°

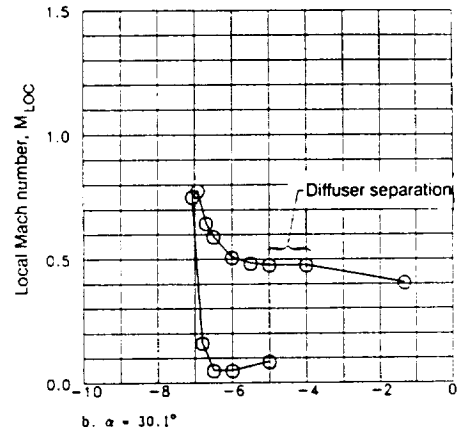

b. α = 30.1°

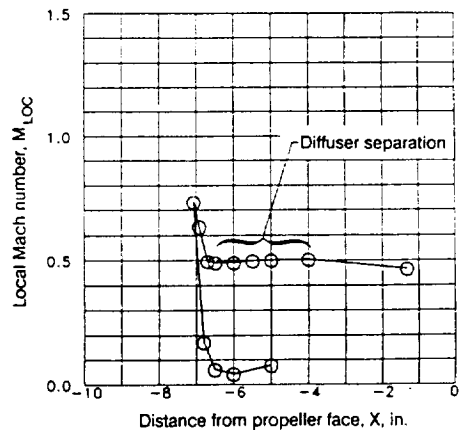

c. α = 32.4°

Fig 10 Inlet Mach number distributions in the midlength inlet showing the development of diffuser separation. Nominal corrected flow, W_c, 30.5 lb/sec.

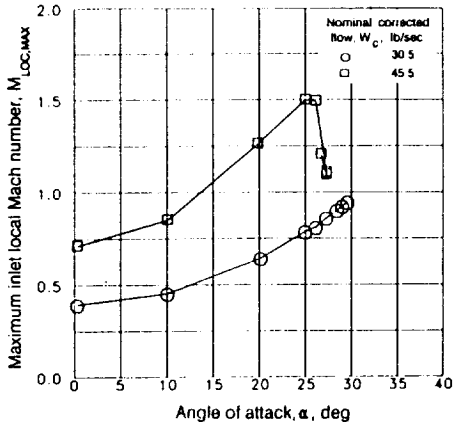

Fig 11 Variation of the maximum inlet local Mach number with angle of attack for the conventional inlet.

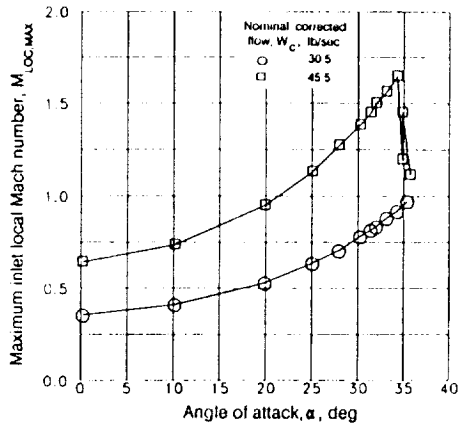

Fig 12 Variation of the maximum inlet local Mach number with angle of attack for the hybrid inlet.

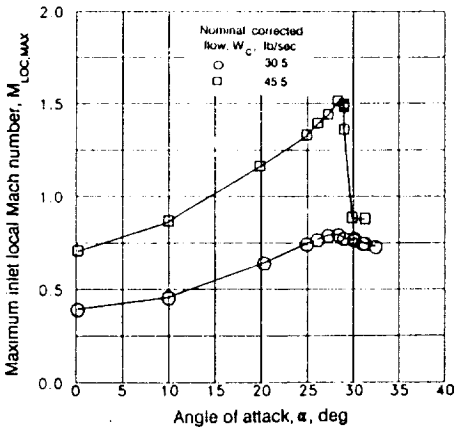

Fig 13 Variation of the maximum inlet local Mach number with angle of attack for the midlength inlet.

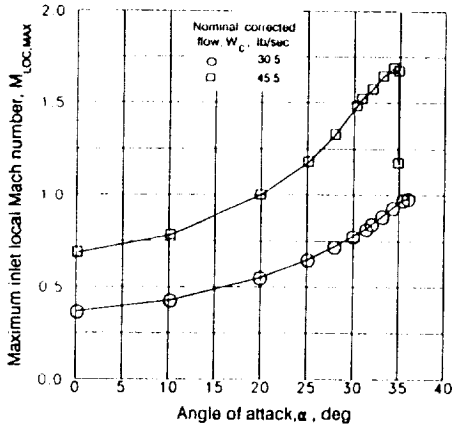

Fig 14 Variation of the maximum inlet local Mach number with angle of attack for the plug inlet.

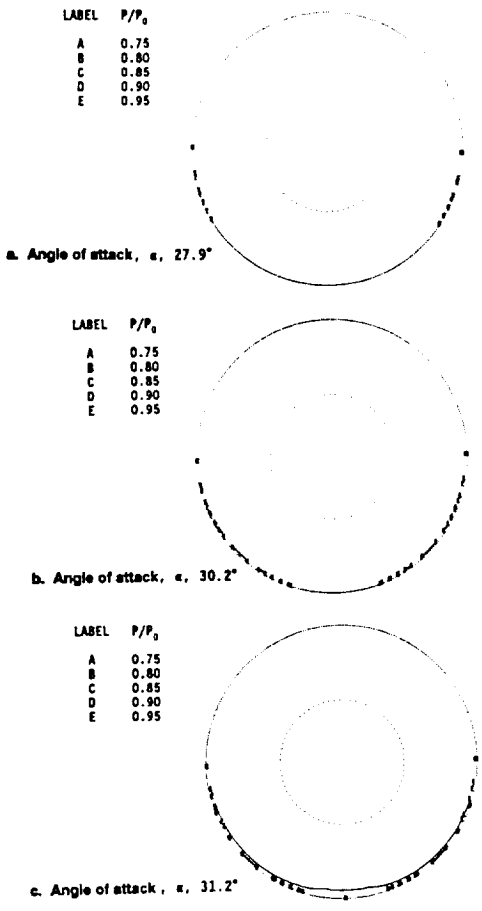

Fig 15 Inlet distortion total pressure contours in the midlength inlet. Nominal corrected flow, W_c, 30.5 lb/sec.

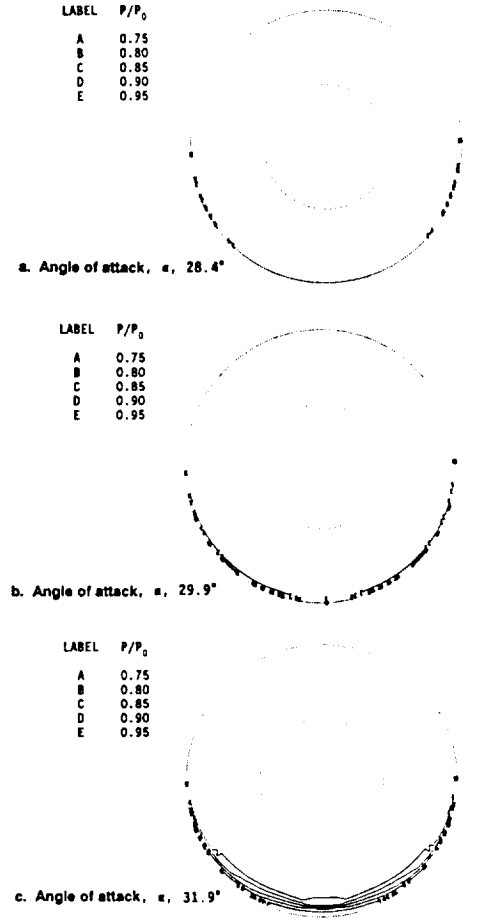

Fig 16 Inlet distortion total pressure contours in the midlength inlet. Nominal corrected flow, W_c, 45.5 lb/sec.

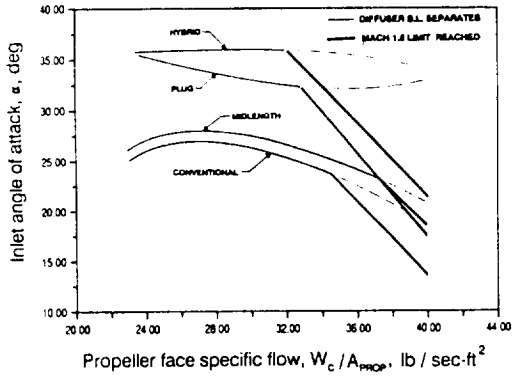

Fig 17 Predicted separation in the four inlets based on simple model. Propeller face flow area, A_{PROP}, 187.7 in^2.

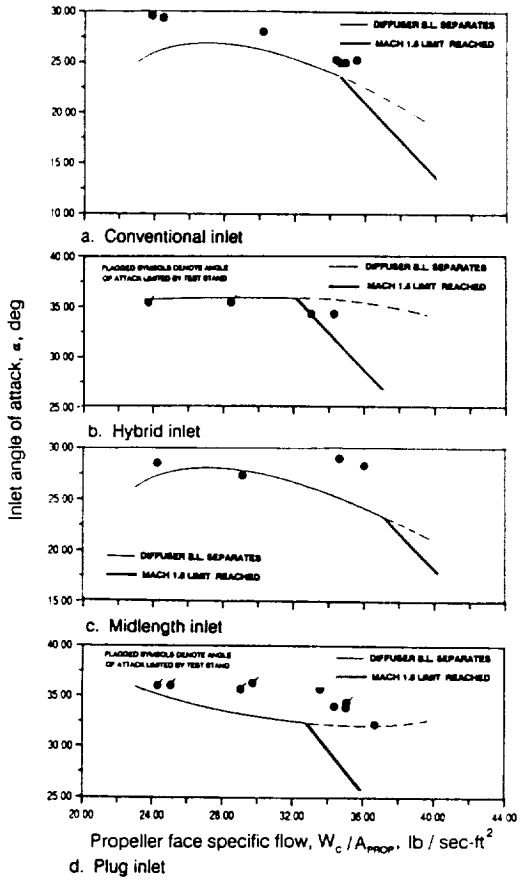

Fig 18 Comparison of predicted separation and observed "onset" of separation for the four inlets. Propeller face flow area, A_{PROP}, 187.7 in^2.

NASA
National Aeronautics and Space Administration

Report Documentation Page

1. Report No.	2. Government Accession No.	3. Recipient's Catalog No.
NASA TM-104428 AIAA-91-3354		

4. Title and Subtitle
Evaluation of Panel Code Predictions With Experimental Results of Inlet Performance for a 17-Inch Ducted Prop/Fan Simulator Operating at Mach 0.2

5. Report Date

6. Performing Organization Code

7. Author(s)
D.R. Boldman, C. Iek, D.P. Hwang, R.J. Jeracki, M. Larkin, and G. Sorin

8. Performing Organization Report No.
E-6261

10. Work Unit No.
535-03-10

9. Performing Organization Name and Address
National Aeronautics and Space Administration
Lewis Research Center
Cleveland, Ohio 44135-3191

11. Contract or Grant No.

13. Type of Report and Period Covered
Technical Memorandum

12. Sponsoring Agency Name and Address
National Aeronautics and Space Administration
Washington, D.C. 20546-0001

14. Sponsoring Agency Code

15. Supplementary Notes
Prepared for the 27th Joint Propulsion Conference cosponsored by the AIAA, SAE, ASME, and ASEE, Sacramento, California, June 22-27, 1991. D.R. Boldman, C. Iek, D.P. Hwang and R.J. Jeracki, NASA Lewis Research Center. M. Larkin and G. Sorin, Pratt and Whitney Aircraft, East Hartford, Connecticut 06108. Responsible person, D.R. Boldman, (216) 433-3692.

16. Abstract
An axisymmetric panel code was used to evaluate the performance of a series of ducted propeller inlets which were designed by P&W Aircraft and tested in the NASA Lewis 9- by 15-Foot Low Speed Wind Tunnel as part of a joint program with P&W Aircraft. Three basic inlets having ratios of shroud length to propeller diameter of 0.2, 0.4, and 0.5 were tested with the P&W ducted prop/fan simulator. A fourth "hybrid" inlet consisting of the shroud from the shortest basic inlet coupled with the spinner from the longest basic inlet was also tested. This latter configuration represented the shortest overall inlet. The simulator duct diameter at the propeller face was 17.25 inches. The short and long spinners provided hub-to-tip ratios of 0.44 at the propeller face. The four inlets were tested at a nominal free stream Mach number of 0.2 and at angles-of-attack from 0° to 35° (upper limit of the model support system). The panel code method incorporated a simple two-part separation model which yielded conservative estimates of inlet separation.

17. Key Words (Suggested by Author(s))
Air intakes; Engine inlets; Panel method; Potential flow; Separation; Shrouded propellers

18. Distribution Statement
Unclassified - Unlimited
Subject Category 02

19. Security Classif. (of the report)	20. Security Classif. (of this page)	21. No. of pages	22. Price*
Unclassified	Unclassified	18	A03

NASA FORM 1626 OCT 86

*For sale by the National Technical Information Service, Springfield, Virginia 22161